Screening Metal Organic Framework-based Mixed Matrix Membranes for CO_2/CH_4 Separations

Ilknur Erucar† and Seda Keskin‡*

†Department of Computational Sciences and Engineering,

Koç University, 34450, Istanbul, Turkey

‡Department of Chemical and Biological Engineering,

Koç University, 34450, Istanbul, Turkey

Submitted to Ind. Eng. Chem. Res.

Abstract

In this study, the challenge of selecting metal organic frameworks (MOFs) as filler particles in high performance mixed matrix membranes (MMMs) was examined using atomistic and continuum modeling. We tested several theoretical permeation models such as Maxwell, modified Maxwell, Bruggeman, Lewis-Nielson, Pal, Felske and modified Felske by comparing the predictions of these models with the experimental data for IRMOF-1/Matrimid and CuBTC/Matrimid MMMs. After identifying the best predicting model, we examined the performance of eighty new MOF-based MMMs composed of ten different MOFs and eight different polymers for CO_2/CH_4 separations. Our results showed that selecting appropriate MOF as filler particles in polymers can result in MMMs with extraordinarily high CO_2 selectivity and CO_2 permeability relative to pure polymer membranes. The methods we introduced in this study will create many opportunities for selecting MOF/polymer combinations for MMMs with useful properties for CO_2 separation applications.

* Corresponding author. Email: skeskin@ku.edu.tr

TOC Graphic

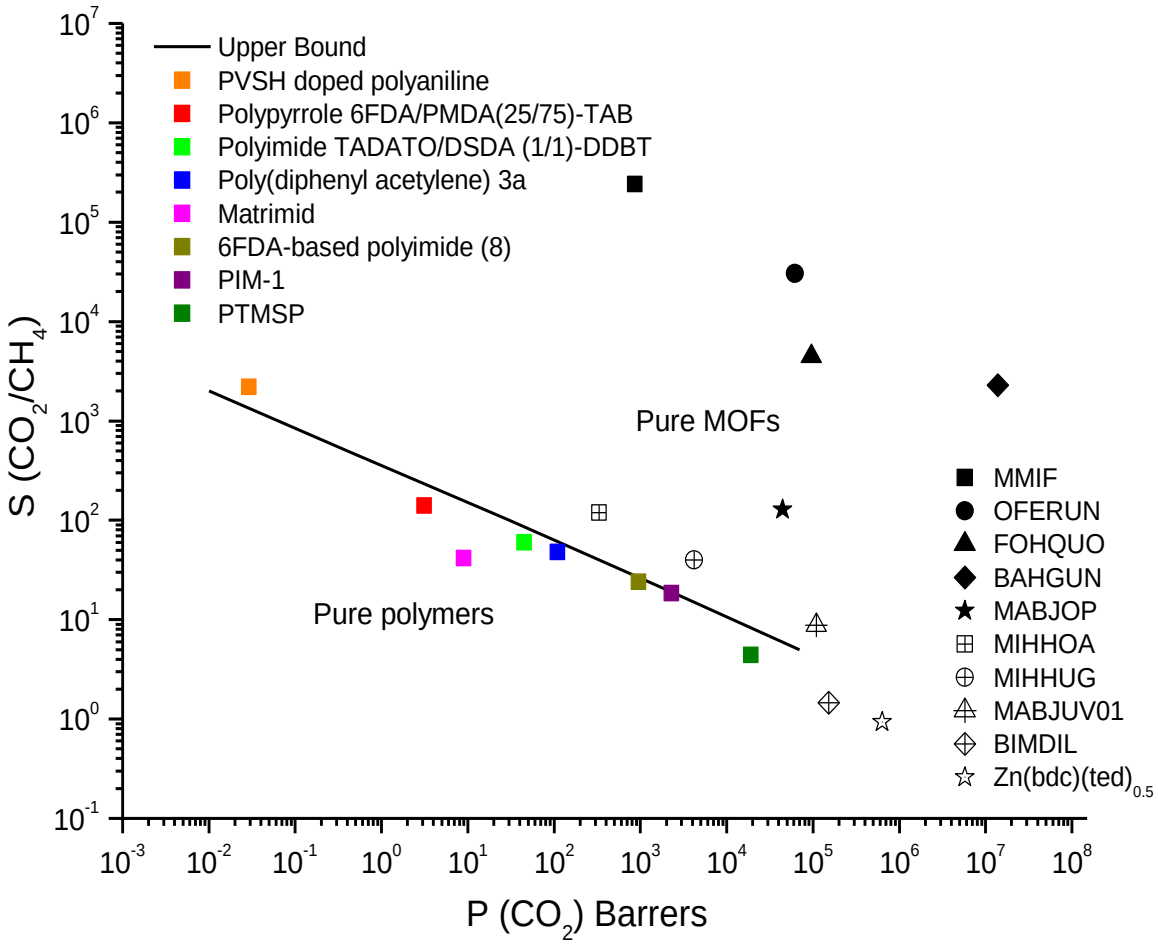
Upper Bound
PVSH doped polyaniline
Polypyrrole 6FDA/PMDA(25/75)-TAB
Polyimide TADATO/DSDA (1/1)-DDBT
Poly(diphenyl acetylene) 3a
Matrimid
6FDA-based polyimide (8)
PIM-1
PTMSP
Pure MOFs
Pure polymers
MMIF
OFERUN
FOHQUO
BAHGUN
MABJOP
MIHHOA
MIHHUG
MABJUV01
BIMDIL
Zn(bdc)(ted)0.5
S (CO2/CH4)
P (CO2) Barrers

1. Introduction:

Development of robust materials as alternatives to polymer membranes to achieve CO_2/CH_4 separations with high gas selectivity and high gas permeability would have important social and economical impacts on mitigation of CO_2 emissions. The current membrane market for CO_2/CH_4 separations is dominated by polymer membranes due to their ease of fabrication and low cost. Unfortunately, polymer membranes have a trade-off between selectivity and permeability. Robeson used large collections of experimental data to demonstrate the inverse relationship between selectivity and permeability of polymer membranes.[1-2] Freeman[3-4] presented a theory showing that the upper bound on membrane performance described by Robeson is a natural consequence of the strong size sieving nature of the stiff chain glassy polymer materials whose properties generally define the upper bound. Identification and development of membranes that can exceed Robeson's upper bound for selectivity and permeability has been the central focus of research in high performance membranes for the past two decades.

Making membranes from non-polymeric materials such as zeolites,[5] carbon molecular sieves[6] and carbon nanotubes[7-8] is one way to overcome the selectivity/permeability trade-off.[9] For example, zeolites DDR and SAPO-34 are known to be highly selective for CO_2 in separation of CO_2/CH_4 mixtures.[10-11] Unfortunately, scale up and high manufacturing costs present fundamental challenges in the commercial implementation of these materials as membranes.[12] The other way to overcome the selectivity/permeability trade-off of polymer membranes is to combine polymers with non-polymeric particles to make composite membranes. These membranes are also called mixed matrix membranes (MMMs) and they present greater promise for short-term commercial implementation. MMMs are heterogeneous membranes in which organic/inorganic fillers are embedded into a polymer matrix. Fabrication of these membranes on large scales can readily be envisioned with relatively minor adaptation of existing commercial technology.[13-14] Numerous MMMs have been reported in the literature with various types of filler particles such as non-porous silica particles,[15] carbon molecular sieves,[16-17] zeolites,[18-21] fullerenes[22] and carbon nanotubes.[23]

In this study, we considered the use of a relatively new family of nanoporous materials, metal organic frameworks (MOFs), as filler particles in MMMs. Metal organic frameworks (MOFs) are a new family of crystalline nanoporous materials with potential in gas storage and gas separation applications due to their well defined pores and large surface areas.[24] MOFs are composed of metal ligand complexes forming vertices of a framework that is connected with

organic linkers. The main advantage of MOFs over well known nanoporous materials such as zeolites is the ability to tune their physical and chemical properties during their synthesis by changing the combination of metal and organic linker groups. Rational combination of different metal ions and organic linkers in the synthesis of MOFs results in materials with various pore size and connectivity, offering theoretically infinite number of possible structures.[25]

Incorporation of MOFs into polymers has started recently. The first MOF-based MMM containing copper (II) biphenyl dicarboxylate triethylenediamine in poly (3-acetoxyethylthiophene) synthesized by Yehia and co-workers[26] showed an enhanced CH_4 selectivity relative to the pure polymer. Car et al.[27] prepared MMMs with two different polymers, poly-dimethylsiloxane and polysulfone, and two MOFs, CuBTC and $Mn(HCOO)_2$, as filler particles in the polymers for separation of CO_2 from N_2 and CH_4. Very slight improvements in the ideal selectivity for CO_2 over N_2 and CH_4 were observed. The slight improvements in ideal selectivity can be due to the leaky interface morphology as recently discussed by Basu et al.[28] Leaks increase the diffusion coefficient of gases especially at higher loadings of particles and therefore selectivity improvement is observed to be lower than expected. Zhang et al.[29] incorporated Cu-BPY-HFS into a Matrimid membrane to study the pure gas permeation of H_2, N_2, O_2, CH_4, and CO_2 as well as the separation of CO_2/CH_4, H_2/CO_2 and CH_4/N_2 mixtures and concluded that both the ideal and mixture selectivity towards CH_4 in MMM is increased due to the affinity of Cu-BPY-HFS towards CH_4. Perez et al.[30] used the most widely studied MOF, IRMOF-1 as filler particles in Matrimid to study the same gas pairs mentioned above. Although IRMOF-1 did not lead to increase in the membrane selectivity, the permeability of the MMM was up to 120% larger than the pure polymer. Adams et al.[31] incorporated CuTPA MOF into polyvinyl acetate and observed that both CO_2 permeability and ideal selectivity were enhanced with MMMs. Diaz et al.[32] used pulse field gradient NMR techniques to study transport of CO_2 in a pristine poly(1,4-phenylene ether-ether-sulfone) membrane and MMMs including ZIF-8 (zeolite imidazolate framework) particles in this polymer. Bae and coworkers[33] used ZIF-90 as filler particles in Ultem, Matrimid and 6FDA-DAM polyimide and measured both pure and mixed gas permeabilities of CO_2 and CH_4 in these membranes. They showed that ZIF-90/6FDA-DAM membranes have unprecedented high performance for CO_2/CH_4 separation and promising CO_2/N_2 separation properties. Basu et al.[34] synthesized CuBTC/Matrimid and CuBTC/Matrimid/polysulphone membranes and measured mixed gas permeation of CO_2/CH_4

and CO_2/N_2 at various compositions through these membranes. They observed an increase both in selectivity and permeance of CO_2 compared to the reference polymer membranes. Hu et al.[35] synthesized CuBTC/polyimide MMMs and reported that H_2 permeance and selectivity increased compared to pure polyimide. In a recent work, four MOF-based MMMs composed of polydimethylsiloxane (PDMS) and filler particles of CuBTC, MIL-47, MIL-53(Al) and ZIF-8 were synthesized and characterized.[36]

Although a high degree of MOF/polymer adhesion as characterized by scanning electron microscopy was found in these early attempts of fabricating MOF-based MMMs, the gas-separation performance of these membranes was not high. This may be due to the several factors defining MMMs' performance such as sieve-in-a-cage morphology, leaky interface morphology, matrix rigidification morphology as discusses in detail in a recent review.[28] In addition to the control of interface morphology, the selection of appropriate MOF/polymer pairs is indispensable for high-performance MMMs. Choosing the appropriate MOF as filler particles in MMM applications for specific separations of interest is a challenge due to the very large number of existing MOF materials. Even if only one polymer is considered, there are hundreds of MOFs that could potentially be used as filler particles. Therefore, theoretical models that can predict polymer/MOF combinations that will have particularly attractive performance are likely to play a critical role in focusing experimental efforts. Keskin and Sholl[37] recently introduced a method that combines atomic simulations with Maxwell permeation model to provide the first quantitative information of MOF-based MMMs. They examined performances of IRMOF-1, IRMOF-8, IRMOF-10, IRMOF-14, CuBTC and Cu(hfipbb) as filler particles in Matrimid and showed that several well known MOFs such as IRMOF-1 and CuBTC can increase the permeability of CO_2 through MMMs relative to the pure polymer membrane but do not improve membrane selectivity, which was in agreement with initial experimental studies. One way to achieve high CO_2 selectivity in CO_2/CH_4 separations is to extend studies to MOFs that show large diffusion-based selectivities for CO_2 over CH_4. Recent studies indicated that MOFs having large cages connected with narrow windows exhibit high diffusion-based selectivities for CO_2, therefore studying these MOFs as filler particles can yield high performance MMMs.[38-39]

In this work, we used several permeation models including Maxwell, modified Maxwell, Bruggeman, Lewis-Nielson, Pal, Felske and modified Felske to examine performances of MOF-based MMMs. We first compared our model predictions with the available experimental data both for pure and mixed gas permeance in MOF-based MMMs. We then

identified the two best predicting permeation models and used them to study ten different MOFs as filler particles in eight different polymers for separation of CO_2 from CH_4. Our calculations identified several promising MOF/polymer combinations among eighty different types of new-MOF based MMMs which achieve high CO_2 selectivity and CO_2 permeability. The results showed that combination of atomic and continuum modeling can help to select the appropriate MOFs as filler particles to obtain MMMs with extraordinary properties for CO_2/CH_4 separations.

2. Computational Details:

2.1 MOFs and Polymers

We considered ten different MOF structures in this study. Eight of these MOFs were chosen from Cambridge Structural Database (CSD) and they are designated by their reference codes (REFCOD) in CSD. These are BAHGUN, BIMDIL, FOHQUO, MABJOP, MABJUV01, MIHHOA, MIHHUG and OFERUN. These materials were chosen to represent MOFs having pore limiting diameters between 3-3.8 Å and large cavity diameters >3.8 Å, which are consistent with the range of pore sizes suggested to give high CO_2 selectivity in CO_2/CH_4 separations.[40] MIHHOA and MIHHUG (MABJOP and MABJUV01) have 1 dimensional pore in y (z) direction, the same metal sites and similar topologies. BAHGUN and BIMDIL have two dimensional and three dimensional pores with the same metal sites. OFERUN represents a three dimensional porous MOF having large cages (11.5 Å) connected with narrow apertures (3.2 Å). This MOF was chosen since previous studies showed that zeolites and MOFs having this type of pore structure can exhibit high selectivity as membranes in CO_2/CH_4 separations.[39,41] We also included two MOFs that we recently studied as pure MOF membranes, MMIF and $Zn(bdc)(ted)_{0.5}$, since the former (latter) was found to have very high (low) CO_2 selectivity.[38,42] Choosing these MOFs, we included a variety of materials having different CO_2 affinities due to their diverse structures. More detailed information on structural properties of the MOFs considered in this work is given in Table S1 of Supplementary Information.

The polymers we considered in this work are the ones which lie along the current Robeson's upper bound[2] for CO_2/CH_4 separations: PVSH doped polyaniline, polypyrrole, polyimide TADATO/DSDA (1/1)-DDBT, poly(diphenyl acetylene) 3a, Matrimid, 6FDA-based polyimide, PIM-1 and PTMSP. Among these polymer, PVSH doped polyaniline represents a polymer which has high CO_2 selectivity but low CO_2 permeability whereas PTMSP represents a polymer with extraordinarily high CO_2 permeability but very low selectivity. Others are a

wide range of polymers that have moderate selectivity/permeability for which incorporating a MOF can yield large performance enhancements.

2.2 Permeation models for MMMs

Designing a MMM-based gas separation process requires knowledge of the permeability of gas species through the continuous phase (the polymer matrix) and the dispersed phase (the filler particles, MOFs). There are several models in the literature to predict the permeation of gas species through MMMs. In this study, we used seven different permeation models: Maxwell, modified Maxwell, Bruggeman, Lewis-Nielson, Pal, Felske and modified Felske. In all of the models considered, we used the experimental data for gas selectivity and gas permeability of polymers since data on a huge range of polymeric membranes has been measured experimentally.[1-2] Similar experimental data is not available for MOFs, and a key ingredient of our results is that the gas permeabilities through MOFs were predicted from detailed atomistic simulations as explained in the following section.

The permeation models can be classified into two: models considering ideal morphology which assumes that there are no defects in the polymer-particle interface (Maxwell, Bruggeman, Lewis-Nielson, Pal) and models considering non-ideal morphology that contains interface voids and polymer rigidification around particles (modified Maxwell, Felske and modified Felske.[43-44] Maxwell model[45] is commonly used to predict gas permeability through MMMs:

$$P_r = \frac{P}{P_m} = \left[\frac{2(1-\phi) + (1+2\phi)\lambda_{dm}}{(2+\phi) + (1-\phi)\lambda_{dm}} \right] \quad (1)$$

In this model, λ_{dm} is the permeability ratio (P_d/P_m), P_d is the permeability of dispersed phase, P_m is the permeability of continuous phase, P_r is the relative permeability, P is the permeability in MOF/polymer MMM and ϕ is the volume fraction of MOF particles. Maxwell model is valid for low to moderate values of volume fractions ($0<\phi<0.2$) since it assumes that nearby particles do not affect the streamlines around particles. This model does not consider packing limit of particles, the effect of particle size distribution, particle shape and aggregation of particles. Bruggeman model[46] is valid for a broader range of ϕ compared to Maxwell model, however it has the same limitations with Maxwell model:

$$P_r^{(1/3)}\left[\frac{\lambda_{dm}-1}{\lambda_{dm}-P_r}\right]=(1-\phi)^{-1} \tag{2}$$

Lewis-Nielson model[47] has a broad range of ϕ, ($0 < \phi < \phi_m$), where ϕ_m is the maximum packing volume fraction of filler particles and assumed to be 0.64 for random close packing of uniform spheres:[43-44,48]

$$P_r=\frac{P}{P_m}=\left[\frac{1+2((\lambda_{dm}-1)/(\lambda_{dm}+2))\phi}{1-((\lambda_{dm}-1)/(\lambda_{dm}+2))\phi\varphi}\right] \tag{3}$$

$$\varphi=1+\left[\frac{(1-\phi_m)}{(\phi_m)^2}\right]\phi \tag{4}$$

Lewis-Nielson model includes morphology effects on permeability since ϕ_m is related to particle size distribution, particle shape and aggregation of particles. The model reduces to Maxwell model when ϕ_m goes to 1.

Pal model[49] also considers the effect of particle size distribution, particle shape and aggregation of particles. This model reduces to Bruggeman model when ϕ_m goes to 1:

$$P_r^{(1/3)}\left[\frac{\lambda_{dm}-1}{\lambda_{dm}-P_r}\right]=\left(1-\frac{\phi}{\phi_m}\right)^{-\phi_m} \tag{5}$$

Modified Maxwell model is based on the two-phase description, the polymer matrix is one phase, the dispersed particles (insert)-interface is the other phase ('pseudo-insert' phase).[50] This model predicts permeability of gases through 'pseudo-insert' phase by using the following expression:

$$P_{eff}=P_I\left[\frac{2(1-\phi_s)+(1+2\phi_s)(P_d/P_I)}{(2+\phi_s)+(1-\phi_s)(P_d/P_I)}\right] \tag{6}$$

where P_{eff} is the effective permeability of the 'pseudo-insert' phase, P_I is the permeability of the interphase, ϕ_s is the volume fraction of the dispersed phase within the 'pseudo-insert' phase. The volume fraction of the dispersed phase can be estimated by using following equation:

$$\phi_s = \frac{\phi_d}{\phi_d + \phi_I} = \frac{{r_d}^3}{(r_d + l_I)^3} \tag{7}$$

Here, ϕ_d is the volume fraction of dispersed phase, ϕ_I is the volume fraction of the interphase, r_d is the insert radius, l_I is the interphase thickness. The permeability in MMM can be then estimated by using the following expression:

$$P_r = \frac{P}{P_m} = \left[\frac{2(1-\phi) + (1+2\phi)(P_{eff} / P_m)}{(2+\phi) + (1-\phi)(P_{eff} / P_m)} \right] \tag{8}$$

Modified Maxwell model is valid for low to moderate values of filler concentration like Maxwell model. At high values of filler concentration ($\phi \to \phi_m$), significant deviation from actual behavior can be observed. Modified Maxwell does not take account for the effect of particle size distribution, particle shape and aggregation of particles.

Felske model[51] considers the dispersed particles as core and the surrounding interfacial layer (rigidified interfacial layer or voids or particle pore blockage) as shell. This model gives almost the same predictions as the modified Maxwell as it reduces to the Maxwell model when δ = 1, that is, when the interfacial layer is absent:

$$P_r = \frac{P}{P_m} = \left[\frac{2(1-\phi) + (1+2\phi)(\beta / \gamma)}{(2+\phi) + (1-\phi)(\beta / \gamma)} \right] \tag{9}$$

$$\begin{aligned} \beta &= (2+\delta^3)\lambda_{dm} - 2(1-\delta^3)\lambda_{\mathrm{lm}} \\ \gamma &= (1+2\delta^3) - (1-\delta^3)\lambda_{dI} \end{aligned} \tag{10}$$

Here, δ is the ratio of outer radius of interfacial shell to core radius, ϕ is the volume fraction of core-shell particles, λ_{lm} is the permeability ratio of P_I/P_m and λ_{dI} is the permeability ratio of P_d/P_I. This model is suitable for low volume fraction of particles.

Modified Felske model was developed to demonstrate permeation behavior in MMMs by considering the morphology and packing factor of particles:

$$P_r = \frac{P}{P_m} = \left[\frac{1 + 2((\beta - \gamma)/(\beta + 2\gamma))\phi}{1 - ((\beta - \gamma)/(\beta + 2\gamma))\phi\rho} \right] \tag{11}$$

This model turns into original Felske model when ϕ_m is equal to 1 and it reduces to Lewis-Nielson model when δ = 1. If both of these parameters are equal to 1, this model gives Maxwell prediction. The values of parameters, ϕ_m , ϕ_s and δ which are required to use in some of the expression listed above were obtained from the recent study of Shimekit et al.[44] and given in Table S2.

The predicted ideal selectivity of the MMMs for a gas pair is simply the ratio of permeabilities of two competing gas components. For a mixture consisting of 2 species, 1 and 2, the selectivity is defined as:

$$S_{1/2} = \frac{P_1}{P_2} \tag{12}$$

2.3 Predicting Gas Permeabilities through MOFs using Atomic Simulations

Atomically detailed modeling has been widely used to examine molecular adsorption and transport in MOFs.[52] In order to predict gas permeabilities through MOFs, atomically detailed simulations were used. Atomic positions of the MOFs were obtained from the experimentally reported crystal files in CSD. We used universal force field (UFF)[53] for the framework atoms. Spherical Lennard-Jones (LJ) 12-6 potentials were used to model CH_4[54] whereas CO_2 was represented as a three site linear molecule and its quadrupole moment was described by a partial charge model.[55] For CO_2 simulations, partial charges were added to the framework atoms using connectivity-based atom contribution (CBAC) method.[56] In this method it is assumed that the atoms with the same bonding connectivity have identical charges in different MOFs. Earlier studies showed that the CBAC charges give nearly identical results to those from quantum mechanical calculations for adsorption isotherms of CO_2.[56-57] More details of atomic simulations can be found in our early studies.[38,42,57-61]

We performed grand canonical Monte Carlo (GCMC) simulations to compute the single component adsorption isotherms of CO_2 and CH_4 in MOFs as a function of gas fugacity. Equilibrium molecular dynamics (EMD) simulations were used to compute the loading dependent corrected diffusivities of the same species when adsorbed as pure gases. The transport diffusivity (D_t) is then defined without any approximation in terms of the corrected diffusivity (D_o) and the thermodynamic correction factor,[62] where the latter is a partial derivative relating the adsorbate concentration, c, and bulk phase fugacity, f. The thermodynamic correction factor is fully defined once the single component adsorption

isotherm is known. The relationship between the transport and corrected diffusivity is given as:

$$D_t(c) = D_o(c) \cdot \frac{\partial \ln f}{\partial \ln c}. \tag{13}$$

Steady state fluxes (J) of species across a MOF crystal are calculated based on Fick's law,[62]

$$J = -D_t(c) \cdot \nabla c \tag{14}$$

where ∇c is the concentration gradient of the adsorbed species based on the difference between the feed and permeate side pressures of the membrane. The gas flux in MOFs is then converted to permeability, P, using pressure drop (Δp), and membrane thickness, L, by[63]

$$P = \frac{J}{\Delta p / L}. \tag{15}$$

For all MOFs except IRMOF-1 and CuBTC, GCMC and EMD simulations were performed at 25°C and at a feed (permeate) pressure of 2 bar (vacuum) to be consistent with the experimental data of the pure polymer membranes. For IRMOF-1 and CuBTC, molecular simulations were performed at 35°C, 2 bar and 35°C, 10 bar, respectively since the experimental data for these membranes was reported at these conditions.

Modeling mixture permeation through MMMs is more complicated than describing pure gas permeation since the gas permeabilities of each species can be affected by competition effects between the two species. We only considered permeation of CO_2/CH_4:35/65 mixtures in CuBTC/Matrimid membranes to make a comparison with the available experimental data on the same membrane. The permeabilities of CO_2/CH_4 mixtures through Matrimid membranes were obtained from the experimental data[34] whereas permeabilities through CuBTC membranes were calculated using molecular simulations and mixing theories. These calculations were performed by predicting adsorption isotherms and transport diffusivities of CO_2/CH_4 mixtures in CuBTC using GCMC simulations and Skoulidas-Sholl-Krishna[64] methods, respectively. Steady state permeance of CO_2/CH_4 mixtures through defect-free CuBTC membranes was calculated by specifying the pressure and composition of the bulk gas mixture on the feed side and the pressure on the permeate side of membrane and finding the flux of each species iteratively. The details of these calculations have been described in

our previous papers.[65-66] After the permeabilities of CO_2/CH_4 mixtures in Matrimid and CuBTC were calculated separately, the permeation models were used to predict the mixture permeabilities for CuBTC/Matrimid MMMs.

3. Results and discussion:

3.1 Comparing predictions of various models with experimental data for MOF-based MMMs

We first compared the predictions of the permeation models with the available experimental measurements for pure gas and mixed gas permeation in order to determine the best predicting permeation model (see Table 1). Figure 1a (1b) shows the comparison of experimental data with model predictions for permeability of CO_2 (CH_4) in IRMOF-1/Matrimid membranes. Permeation of CO_2 and CH_4 through pure Matrimid and IRMOF-1/Matrimid membranes were measured by Perez et al.[30] The three data points for each model represent the permeability of species in MMMs as the weight per cent of IRMOF-1 increases from 0.1 to 0.3 in the membrane. Pal, Bruggeman, Lewis-Nielson, Maxwell models overestimated both CO_2 and CH_4 permeability data compared to the experimental measurements. The modified Maxwell, Felske and modified Felske models gave better predictions relative to other models. The good agreement between the predictions of these models and the experimental data indicates that these models are appropriate for loadings at least as high as the IRMOF-1 based membranes reported by Perez et al.[30]

In order to be more precise in choosing the best model to predict the performance of new MOF-based MMMs, we calculated the percentage average absolute relative error (AARE%) values for CO_2 and CH_4 permeation data by using $AARE\% = \frac{100}{N}\sum_{i=1}^{N}\left|\frac{P_i^{cal} - P_i^{\exp}}{P_i^{\exp}}\right|$ where P_i^{cal}, $P_i^{\exp}$ and N are permeability calculated by models, permeability measured by experiments and number of data points, respectively. The AARE% values for CO_2 and CH_4 in IRMOF-1/Matrimid membranes are given in Table 2. The estimated AARE% values of the permeation models considering ideal morphology concept were ordered as follows: Pal model > Bruggeman model > Lewis–Nielsen model > Maxwell model. The other models consider interfacial morphologies and AARE% values of these models were in the following order: modified Maxwell model > Felske model > modified Felske model.

Figure 1c shows the mixed gas permeabilities of CO_2/CH_4:35/65 mixture through CuBTC/Matrimid MMMs at 35°C and 10 bar. The predictions of Maxwell and modified

Felske models were again found to be in a better agreement with the experimental measurements of Basu et al.[34] compared to the other models. According to these results, we chose Maxwell model among the models based on ideal morphology concept and modified Felske model among the models considering interfacial morphologies to make predictions for gas permeation through new MOF-based MMMs.

3.2 Predicting selectivity and permeability of new MOF-based MMMs

The main outcome of the calculations described above is that the Maxwell and Modified Felske models show good agreement with the available experimental data for IRMOF-1/Matrimid and CuBTC/Matrimid membranes which suggests that a combination of various MOF/polymer can be also studied with these models to estimate the gas permeabilities prior to the fabrication of new MMMs. With this aim, we investigated the performance of new MOF-based MMMs which include BAHGUN, BIMDIL, FOHQUO, MABJOP, MABJUV01, MIHHOA, MIHHUG and OFERUN as filler particles. Figure 2 shows the CO_2 selectivity and CO_2 permeability of pure polymers and pure MOFs. The CO_2 selectivity/permeability performances of MOFs were calculated using atomic simulations as described above. Values for polymers were taken from Robeson's large experimental data collection and the line in Figure 2 shows the upper bound established for polymer membranes in CO_2/CH_4 separations.[2] Among all polymers and MOFs, MMIF has the highest CO_2/CH_4 selectivity because diffusion of CO_2 is rapid in MMIF whereas CH_4 cannot diffuse due to the large energy barrier experienced at the narrow pore openings as discussed in detail in a recent work.[38] BAHGUN has the highest CO_2 permeability ($>10^7$ Barrers) due to its highly porous structure. BIMDIL and $Zn(bdc)(ted)_{0.5}$ have the lowest CO_2 selectivities, 1.5 and 0.9, respectively. Except these two, all MOFs are above the upper bound and they show better selectivity or permeability (or both) than pure polymer membranes. This figure hints that when used as filler particles in MMMs all of these MOFs will potentially bring an enhancement either in permeability or selectivity or in both. For example, MMIF and OFERUN (BIMDIL and MABJUV01) are expected to increase CO_2 selectivity (CO_2 permeability) of polymers if they are embedded into polymers as fillers.

Figures 3 shows predicted CO_2 selectivity and permeability of MOF-based MMMs for CO_2/CH_4 separations. Results for MMIF/polymer, MABJOP/polymer and BIMDIL/polymer membranes were presented since MMIF, MABJOP and BIMDIL exhibit high selectivity/low permeability, mediocre selectivity/high permeability and low selectivity/high permeability for CO_2, respectively. Similar plots for other MOF-based MMMs (BAHGUN, FOHQUO,

MABJUV01, MIHHOA, MIHHUG and OFERUN) are given in the Supplementary Information. The stars in Figure 3a,c,e (Figure 3b,d,f) represent predictions of Maxwell model (modified Felske model) for selectivity/permeability performances of MMMs where volume fraction of the filler particles increases from 0.1 to 0.5.

Incorporation of MMIF enhances both selectivity and permeability of polypyrrole, polyimide, poly(diphenyl acetylene) and Matrimid since MMIF has higher selectivity/permeability compared to these polymers. Figure 3a shows that pure Matrimid has a CO_2 selectivity of 41.7 (CO_2 permeability of 9 Barrers) whereas MMIF/Matrimid membrane has a CO_2 selectivity of 150.7 (CO_2 permeability of 20.1 Barrers) at a filler volume fraction of 0.3. Since MMIF has lower permeability than polymers PTMSP and PIM-1, selectivity increase in these polymers was obtained at the expense of permeability reduction. For example, pure PTMSP has a CO_2 selectivity of 4.42 and CO_2 permeability of 19000 Barrers, whereas MMIF/PTMSP membrane shows a CO_2 selectivity of 4.59 at a reduced permeability of 12000 Barrers. Figures 3a-b summarize how a MOF exhibiting high CO_2 selectivity/low CO_2 permeability can change the performances of various polymers in CO_2/CH_4 separations. Comparing Figure 3a with 3b indicates that the predictions of modified Felske model is less than those of Maxwell model both for permeability and selectivity. For example, Maxwell model predicts selectivity of MMIF/Matrimid membranes between 64 and 387 for a volume fraction range of 0.1-0.5 whereas modified Felske model's predictions are between 51 and 135 under the same conditions. In other words, the model considering ideal morphology which assumes that there are no defects in the polymer-particle interface gives more optimistic results than the model which considers non-ideal morphology that contains interface voids and polymer rigidification around particles.

Using MABJOP as filler particles in polymers enhances both selectivity and permeability of PTMSP, PIM-1 and 6FDA-based polymide as shown in Figures 3c-d. A MMM having MABJOP with a volume fraction of 0.3 can carry pure PTMSP membrane above the upper bound by increasing its selectivity from 4.42 to 8.88. Since the selectivity of MABJOP is not significantly better than the other polymers such as Matrimid, polypyrrole, poly(diphenyl acetylene), only permeability enhancement was observed in these MMMs which can be attributed to highly porous structure of the MABJOP. Figures 3c-d represent the performances of various MMMs consisted of a MOF with mediocre selectivity/high permeability as a filler particle. Similar to the previous comment, the predictions of modified Felske model both in selectivity and permeability are less than the predictions of Maxwell model, therefore higher

volume fractions of filler particles are required to carry MMMs above Robeson's curve according to modified Felske model.

Performances of MMMs composed of BIMDIL and polymers are shown in Figures 3e and 3f. BIMDIL has very high permeability (>10^5 Barrers) compared to pure polymers. The CO_2 selectivity of BIMDIL is very low (1.5) because the diffusion rate of CO_2 and CH_4 in the pores are very similar (~10^{-5} cm^2/s). One can easily anticipate that BIMDIL is not a good candidate as filler particles to improve the selectivity of polymer membranes. One extreme case is the MMM with the polymer PTMSP. Since this polymer has also low selectivity like BIMDIL, permeability increase in the MMM was obtained at the expense of selectivity reduction. Figures 3e-f show that using low selectivity/high permeability MOFs in polymers only increases permeability without making any significant change (or a slight decrease) in selectivity.

The three MOFs we discussed above underlines the importance of polymer/MOF matching in the MMM applications and the trends that are evident in Figure 3 will be very useful in developing MOF-based MMMs. If the pure polymer membrane has a high selectivity for CO_2 but low CO_2 permeability such as PVSH doped polyaniline, adding a MOF can enhance the membrane's permeability slightly with little or no change in the membrane's selectivity. In this limit, the identity of the MOF appears to be unimportant, it can be very selective like MMIF or it can have very low selectivity like BIMDIL. Another extreme example of polymer performance is a polymer that is very permeable but has a little selectivity (PTMSP). For this type of polymers, the identity of the MOF used in a MMM plays a critical role. A permeable but unselective MOF such as BIMDIL can yield a MMM with a lower selectivity but a higher permeability than the pure polymer. A highly selective MOF such as MMIF, in contrast, increases the selectivity of a MMM but decreases the CO_2 permeability. Figure 3 most importantly showed that there is a wide range of polymers that have moderate selectivity and moderate permeability for which adding an appropriate MOF can yield large performance enhancements and carry the polymer above the upper bound. In order to realize this result, it is critical to use a highly selective MOF such as MMIF, OFERUN, FOHQUO, BAHGUN rather than unselective MOFs such as BIMDIL, $Zn(bdc)(ted)_{0.5}$, MABJUV01 (see Figure S1).

Since there are hundreds of different MOF structures in CSD, developing methods for making accurate predictions in MOF selection without performing very detailed calculations would be very valuable. Relating microscopic characteristics like gas diffusion in MOFs' pores with

macroscopic quantities like gas permeability through MOFs can be helpful in identifying promising materials prior to carrying out extensive calculations. With this aim, we examined the relation between energy barrier to CO_2 permeation and CO_2 permeability in MOFs. Atomic simulations provided molecular diffusivities of CO_2 and CH_4 in each MOF and we used these values to extract the energy barrier to diffusion using a simple transition state expression, $E_{trans}^{CO_2} = -\ln\left(\frac{n \cdot D^{CO_2}}{\upsilon \cdot a^2}\right) \cdot k_B \cdot T$. In this expression, $E_{trans}^{CO_2}$ is the transition energy barrier to diffusion of CO_2, n is the dimension of the pores (1 or 2 or 3), υ is the pre-exponential factor (taken to be 10^{12} s^{-1}), D^{CO_2} is the diffusivity of CO_2 calculated from EMD simulations, a is the cage-to-cage distance in MOFs, k_B is the Boltzmann constant and T is temperature.

Figure 4a shows the CO_2 permeabilities in MOFs as a function of energy barrier to diffusion. Since permeability is a function of diffusivity (see Eqs. 14 and 15), it decreases as the energy barrier to diffusion is increased. The materials which exhibit lower transition energy barrier to CO_2 molecules in their pores are the ones with higher permeabilities. These are BAHGUN, $Zn(bdc)(ted)_{0.5}$ and BIMDIL ($P_{CO2}>10^5$ Barrers). However, a high permeability alone is of limited value if the membrane cannot separate two components with high efficiency. Earlier we showed that $Zn(bdc)(ted)_{0.5}$ and BIMDIL are not selective for CO_2 over CH_4 even though they have large CO_2 permeabilities. One can conclude by performing EMD simulations that MOFs having low energy barrier to CO_2 diffusion can be good candidates to be used as filler particles for polymers like PVSH doped polyaniline to enhance the permeability without decreasing selectivity.

Both high selectivity and high gas permeability are required to lower the cost of large scale membrane-based gas separation processes. Figure 4b shows the relation between CO_2 selectivity and energy barrier to CO_2 permeation. Correlations can be observed for two groups of MOFs, one for MOFs with high CO_2 selectivities, and one for MOFs with low-mediocre CO_2 selectivities. In each group, as the energy barrier to diffusion of CO_2 is increased, the CO_2 selectivity also increases. This can be explained with the following discussion: As the energy barrier to gas diffusion increases, the permeability of gases decreases. Since CH_4 is a larger molecule than CO_2, it experiences higher energy barrier than CO_2 in the same pores of MOFs under the same conditions. Due to the more pronounced decrease in CH_4 permeability compared to CO_2 permeability, selectivity favors CO_2 over CH_4. To summarize, Figures 4a-b

suggest that measuring energy barrier to diffusion of adsorbates using EMD simulations can hint if the selectivity/permeability performance of MOFs will be useful for MMM applications prior to extensive calculations.

4. Conclusions:

MOF-based MMMs have great potential for energy efficient gas separation. Initial experimental studies reported that there is a good compatibility between MOFs and polymers and fabricating MOF-based MMM is relatively straightforward.[30] Some recent studies in contrast reported poor polymer-filler particle interactions and possible solutions to this problem such as post-treatments to improve the attachment between the polymer matrix and the surface of filler particles were reviewed.[28] In this study, we showed that methods based on combination of atomistic and continuum modeling can successfully examine the performance of MOF/polymer MMMs. Our results indicated that choice of MOFs as filler particles and matching of appropriate MOF/polymer materials is of importance to obtain high performance membranes.

Our previous work on MMMs illustrated that a MOF/polymer combination with excellent separation properties for one gas separation may have less exciting properties for other gas separations.[37] For example, MMIF was identified as a material having strong diffusion-based selectivity for CO_2 over CH_4 due to very slow diffusion of the latter in the narrow pores which are similar in size to CH_4.[38] This study showed that addition of MMIF into polymers as filler particles enhances selectivity of pure polymers. It can be anticipated that MMIF cannot show a high CO_2 selectivity for CO_2/H_2 separations since the difference in transport rates of these two molecules is expected to be a lot lower than the one between CO_2 and CH_4.

Our calculations for pure MOFs described idealized membranes that are made from defect-free single crystals of MOFs. This situation is, of course, not practical to consider for the fabrication of real membranes for practical applications. Understanding the properties of these idealized materials, however, is useful for considering which MOFs from the huge numbers of materials would be worthwhile targets for experimental efforts in MMMs. The results of this work indicate that MOF-based MMMs have enormous potential in practical gas separation applications provided that methods such as those we have introduced above are used to select good material combinations for the desired applications.

Acknowledgment: Financial support provided by the European Commission Marie Curie International Re-integration Grant FP7-PEOPLE-2010-RG (COMMOF-268142) is gratefully acknowledged.

Supporting Information Available: Structural information and gas permeation properties of MOFs, parameters of the permeation models used for predicting permeability of IRMOF-1/Matrimid membranes, Maxwell and modified Felske model predictions for CO_2 selectivity and permeability of MMMs having OFERUN, FOHQUO, BAHGUN, MIHHOA, MIHHUG, MABJUV01 and $Zn(BDC)(TED)_{0.5}$ as filler particles. This material is available free of charge via the Internet at http://pubs.acs.org.

References:

(1) Robeson, L. M. Correlation of Separation Factor Versus Permeability for Polymeric Membranes. *J. Membr. Sci.* **1991**, *62*, 165.

(2) Robeson, L. M. The Upper Bound Revisited. *J. Membr. Sci.* **2008**, *320*, 390.

(3) Freeman, B. D. Basis of Permeability/Selectivity Tradeoff Relations in Polymeric Gas Separation Membranes. *Macromolecules* **1999**, *32*, 375.

(4) Robeson, L. M.; Freeman, B. D.; Paul, D. R.; Rowe, B. W. An Empirical Correlation of Gas Permeability and Permselectivity in Polymers and Its Theoretical Basis. *J. Membr. Sci.* **2009**, *341*, 178.

(5) Snyder, M. A.; Tsapatsis, M. Hierarchical Nanomanufacturing: From Shaped Zeolite Nanoparitcles to High-Performance Separation Membranes. *Angew. Chem. Int. Ed.* **2007**, *46*.

(6) Shiflett, M. B.; Foley, H. C. Ultrasonic Deposition of High-Selectivity Nanoporous Carbon Membranes. *Science* **1999**, *285*, 1902.

(7) Hinds, B. J.; Chopra, N.; Rantell, T.; Andrews, R.; Gavalas, V.; Bachas, L. Aligned Multiwalled Carbon Nanotube Membranes. *Science* **2004**, *303*, 62.

(8) Skoulidas, A. I.; Ackerman, D. M.; Johnson, J. K.; Sholl, D. S. Rapid Transport of Gases in Carbon Nanotubes. *Phys. Rev. Lett.* **2002**, *89*, 185901.

(9) Kariduraganavar, M. Y.; Varghese, J. G.; Choudhari, S. K.; Olley, R. H. Organic−Inorganic Hybrid Membranes: Solving the Trade-Off Phenomenon between Permeation Flux and Selectivity in Pervaporation. *Ind. Eng. Chem. Res.* **2009**, *48*, 4002.

(10) Tomita, T.; Nakayama, K.; Sakai, H. Gas Separation Characteristics of DDR Type Zeolite Membrane. *Micro. Meso. Mater.* **2004**, *68*, 71.

(11) Li, S. G.; Falconer, J. L.; Noble, R. D. Improved SAPO-34 Membranes for CO_2/CH_4 Separations. *Adv. Mat.* **2006**, *18*, 2601.

(12) Julbe, A. In *Introduction to Zeolite Science and Practice*; 3rd ed.; J. Cejka, H. B., A. Corma, F. Schuth, Ed.; Elsevier 2007.

(13) Zimmerman, C. M.; Singh, A.; Koros, W. J. Tailoring Mixed Matrix Composite Membranes for Gas Separations. *J. Membr. Sci.* **1997**, *137*, 145.

(14) Mahajan, R.; Koros, W. J. Factors Controlling Successful Formation of Mixed-Matrix Gas Separation Materials. *Ind. Eng. Chem. Res.* **2000**, *39*, 2692.

(15) Merkel, T. C.; Freeman, B. D.; Spontak, R. J.; He, Z.; Pinnau, I.; Meakin, P.; Hill, A. J. Ultrapermeable, Reverse-Selective Nanocomposite Membranes. *Science* **2002**, *296*, 519.

(16) Vu, D. Q.; Koros, W. J.; Miller, S. J. Mixed Matrix Membranes Using Carbon Molecular Sieves. I. Preparation and Experimental Results. *J. Membr. Sci.* **2003**, *211*, 311.

(17) Das, M.; Perry, J. D.; Koros, W. J. Gas-Transport-Property Performance of Hybrid Carbon Molecular Sieve−Polymer Materials. *Ind. Eng. Chem. Res.* **2010**, *49*, 9310.

(18) Moore, T. T.; Koros, W. J. Sorption in Zeolites Modified for Use in Organic−Inorganic Hybrid Membranes. *Ind. Eng. Chem. Res.* **2008**, *47*, 591.

(19) Hennepe, H. J. C.; Boswerger, W. B. F.; Bargeman, D.; Mulder, M. H. V.; Smolders, C. A. Zeolite-Filled Silicon Rubber Membranes—Experimental Determination of Concentration Profiles. *J. Membr. Sci.* **1994**, *89* 185.

(20) Okumus, E.; Gurkan, T.; Yilmaz, L. Development of a Mixed Matrix Membrane for Pervaporation. *Sep. Sci. Technol.* **1994**, *29*, 2451.

(21) Vankelecom, I. F. J.; Dotremont, C.; Morobe, M.; Uytterhoeven, J. B.; Vandecasteele, C. Zeolite-Filled Pdms Membranes. 1. Sorption of Halogenated Hydrocarbons. *J. Phys. Chem. B* **1997**, *101*, 2154.

(22) Chung, T.; Chan, S.; Wang, R.; Lu, Z.; He, C. Characterization of Permeability and Sorption in Matrimid/C60 Mixed Matrix Membranes. *J. Membr. Sci.* **2003**, *211*, 91.

(23) Qiu, S.; Wu, L.; Shi, G.; Zhang, L.; Chen, H.; Gao, C. Preparation and Pervaporation Property of Chitosan Membrane with Functionalized Multiwalled Carbon Nanotubes. *Ind. Eng. Chem. Res.* **2010**, *49*, 11667.

(24) Eddaoudi, M.; Li, H.; Yaghi, O. M. Highly Porous and Stable Metal-Organic Frameworks: Structure Design and Sorption Properties. *J. Am. Chem. Soc.* **2000**, *122*, 1391.

(25) Banerjee, R.; Furukawa, H.; Britt, D.; Knobler, C.; O'Keeffe, M.; Yaghi, O. M. Control of Pore Size and Functionality in Isoreticular Zeolitic Imidazolate Frameworks and Their Carbon Dioxide Selective Capture Properties. *J. Am. Chem. Soc.* **2009**, *131*, 3875.

(26) Yehia, H.; Pisklak, T. J.; Ferraris, J. P.; Balkus, K. J.; Musselman, I. H. Methane Facilitated Transport Using Copper(II) Biphenyl Dicarboxylatetriethylenediamine/Poly(3-Acetoxyethylthiophene) Mixed Matrix Membranes. *Polym. Prepr.* **2004**, *45* 35.

(27) Car, A.; Stropnik, C.; Peinemann, K. V. Hybrid Membrane Materials with Different Metal-Organic Frameworks (MOFs) for Gas Separation. *Desalination* **2006**, *200*, 424.

(28) Basu, S.; Khan, A. L.; A.Cano-Odena; Liub, C.; Vankelecom, I. F. J. Membrane-Based Technologies for Biogas Separations. *Chem. Soc. Rev.* **2010**, *39*, 750.

(29) Zhang, Y.; Musselman, I. H.; Ferraris, J. P.; Balkus, K. J. Gas Permeability Properties of Matrimid® Membranes Containing the Metal-Organic Framework Cu–BPY-HFS. *J. Membr. Sci.* **2008**, *313*, 170.

(30) Perez, E. V.; Balkus, K. J.; Ferraris, J. P.; Musselman, I. H. Mixed-Matrix Membranes Containing MOF-5 for Gas Separations. *J. Membr. Sci.* **2009**, *328*, 165.

(31) Adams, R.; Carson, C.; Ward, J.; Tannenbaum, R.; Koros, W. Metal Organic Framework Mixed Matrix Membranes for Gas Separations. *Micro. Meso. Mater.* **2010**, *131*, 13.

(32) Diaz, K.; Garrido, L.; Lopez-Gonzalez, M.; del Castillo, L. F.; Riande, E. CO2 Transport in Polysulfone Membranes Containing Zeolitic Imidazolate Frameworks as Determined by Permeation and PFG NMR Techniques. *Macromolecules* **2010**, *43*, 316.

(33) Bae, T.-H.; Lee, J. S.; Qiu, W.; Koros, W. J.; Jones, C. W.; Nair, S. A High-Performance Gas-Separation Membrane Containing Submicrometer-Sized Metal–Organic Framework Crystals. *Angew. Chem. Int. Ed.* **2010**, *49*, 9863.

(34) Basu, S.; Cano-Odena, A.; Vankelecom, I. F. J. Asymmetric Matrimid/[$Cu_3(Btc)_2$] Mixed Matrix Membranes for Gas Separations. *J. Memb. Sci.* **2010**, *362*.

(35) Hu, J.; Cai, H.; Ren, H.; Wei, Y.; Xu, Z.; Liu, H.; Hu, Y. Mixed-Matrix Membrane Hollow Fibers of $Cu_3(Btc)_2$ MOF and Polyimide for Gas Separation and Adsorption. *Ind. Eng. Chem. Res.* **2010**, *49*, 12605.

(36) Basu, S.; Maes, M.; A.Cano-Odena; Alaerts, L.; Vos, D. E. D.; Vankelecom, I. F. J. Solvent Resistant Nanofiltration (Srnf) Membranes Based on Metal-Organic Frameworks. *J. Memb. Sci.* **2009**, *344*, 190.

(37) Keskin, S.; Sholl, D. S. Selecting Metal Organic Frameworks as Enabling Materials in Mixed Matrix Membranes for High Efficiency Natural Gas Purification. *Energy Environ. Sci.* **2010**, *3*, 343.

(38) Keskin, S. High CO_2 Selectivity of A Microporous Metal-Imidazolate Framework: A Molecular Simulation Study. *Ind. Eng. Chem. Res.* **2011**, *50*, 8230.

(39) Watanabe, T.; Keskin, S.; Nair, S.; Sholl, D. S. Computational Identification of a Metal Organic Framework for High Selectivity Membrane-Based Gas Separations. *Phys. Chem. Chem. Phys.* **2009**, *11*, 11389.

(40) Haldoupis, E.; Nair, S.; Sholl, D. S. Efficient Calculation of Diffusion Limitations in Metal Organic Framework Materials:A Tool for Identifying Materials for Kinetic Separations. *J. Am. Chem. Soc.* **2010**, *132*, 7528.

(41) Jee, S.-E.; Sholl, D. S. Carbon Dioxide and Methane Transport in DDR Zeolite: Insights from Molecular Simulations into Carbon Dioxide Separations in Small Pore Zeolites. *J. Am. Chem. Soc.* **2009**, *131* 7896.

(42) Erucar, I.; Keskin, S. Separation of CO_2 Mixtures Using $Zn(Bdc)(Ted)_{0.5}$ Membranes and Composites: A Molecular Simulation Study. *J. Phys. Chem. C* **2011**, *15*, 13637.

(43) Aroon, M. A.; Ismail, A. F.; Matsuura, T.; Montazer-Rahmati, M. M. Performance Studies of Mixed Matrix Membranes for Gas Separation: A Review. *Sep. Purify. Tech.* **2010**, *75*, 229.

(44) Shimekit, B.; Mukhtara, H.; Murugesan, T. Prediction of the Relative Permeability of Gases in Mixed Matrix Membranes. *J. Memb. Sci.* **2011**, *373*, 152.

(45) Maxwell, J. C. *A Treatise on Electricity and Magnetism*; Dover Publications: New York, 1954.

(46) Bruggeman, D. A. G. Berechnung Verschiedener Physikalischer Konstanten Von Heterogenen Substanzen. I. Dielektrizitatskonstanten Und Leitfahigkeiten Der Mischkorper Aus Isotropen Substanzen. *Ann. Phys.(Leipzig)* **1935**, *1935*, 636.

(47) Lewis, T. B.; Nielsen, L. E. Dynamic Mechanical Properties of Particulate-Filled Composites. *J. Appl. Polym. Sci.* **1970**, *14*, 1449.

(48) Pal, R. Permeation Models for Mixed Matrix Membranes. *J. Colloid Interface Sci.* **2008**, *317*, 191.

(49) Pal, R. New Models for Thermal Conductivity of Particulate Composites. *J. Reinf. Plast. Compos.* **2007**, *26*, 643.

(50) Moore, T. T.; Mahajan, R.; Vu, D. Q.; Koros, W. J. Hybrid Membrane Materials Comprising Organic Polymers with Rigid Dispersed Phases. *AIChE J.* **2004**, *50*.

(51) Felske, J. D. Effective Thermal Conductivity of Composite Spheres in a Continuous Medium with Contact Resistance. *Int. J. Heat Mass Transfer.* **2004**, *47*, 3453.

(52) Keskin, S.; Liu, J.; Rankin, R. B.; Johnson, J. K.; Sholl, D. S. Progress, Opportunities, and Challenges for Applying Atomically Detailed Modeling to Molecular Adsorption and Transport in Metal-Organic Framework Materials. *Ind. Eng. Chem. Res.* **2009**, *48*, 2355.

(53) Rappe, A. K.; Casewit, C. J.; Colwell, K. S.; Goddard, W. A.; Skiff, W. M. UFF, a Full Periodic Table Force Field for Molecular Mechanics and Molecular Dynamics Simulations. *J. Am. Chem. Soc.* **1992**, *114*, 10024.

(54) Martin, M. G.; Siepmann, J. I. Transferable Potentials for Phase Equilibria. 1. United-Atom Description of N-Alkanes. *J. Phys. Chem. B* **1998**, *102*, 2569.

(55) Hirotani, A.; Mizukami, K.; Miura, R.; Takaba, H.; Miya, T.; Fahmi, A.; Stirling, A.; Kubo, M.; Miyamota, A. Grand Canonical Monte Carlo Simulation of the Adsorption of CO_2 on Silicalite and NaZSM-5. *Appl. Surf. Sci.* **1997**, *120*, 81.

(56) Xu, Q.; Zhong, C. A General Approcah for Estimating Framework Charges in Metal Organic Frameworks. *J. Phys. Chem. C* **2010**, *114*, 5035.

(57) Keskin, S. Atomistic Simulations for Adsorption, Diffusion, and Separation of Gas Mixtures in Zeolite Imidazolate Frameworks. *J. Phys. Chem. C* **2011**, *115*, 800.

(58) Keskin, S. Molecular Simulation Study of CH_4/H_2 Mixture Separations Using Metal Organic Framework Membranes and Composites. *J. Phys. Chem. C* **2010**, *114*, 13047.

(59) Keskin, S. Comparing Performance of CPO and IRMOF Membranes for Gas Separations Using Atomistic Models. *Ind. Eng. Chem. Res.* **2010**, *49*, 11689.

(60) Liu, J.; Keskin, S.; Sholl, D.; Johnson, J. K. Molecular Simulations and Theoretical Predictions for Adsorption and Diffusion of CH_4/H_2 and CO_2/CH_4 Mixtures in ZIF-68 and ZIF-70. *J. Phys. Chem. C* **2011**, *115*, 12560.

(61) Atci, E.; Erucar, I.; Keskin, S. Adsorption and Transport of CH_4, CO_2, H_2 Mixtures in a Bio-MOF Material from Molecular Simulations. *J. Phys. Chem. C* **2011**, *115* 6833.

(62) Sholl, D. S. Understanding Macroscopic Diffusion of Adsorbed Molecules in Crystalline Nanoporous Materials Via Atomistic Simulations. *Acc. Chem. Res.* **2006**, *39*, 403.

(63) Kesting, R. E.; Fritzsche, A. K. *Polymeric Gas Separation Membranes*; John Wiley & Sons, Inc.: New York, 1993.

(64) Skoulidas, A. I.; Sholl, D. S.; Krishna, R. Correlation Effects in Diffusion of CH_4/CF_4 Mixtures in MFI Zeolite. A Study Linking MD Simulations with the Maxwell-Stefan Formulation. *Langmuir* **2003**, *19*, 7977.

(65) Keskin, S.; Liu, J.; Johnson, J. K.; Sholl, D. S. Atomically-Detailed Models of Gas Mixture Diffusion through CuBTC Membranes. *Micropor. Mesopor. Mater.* **2009**, *125*, 101.

(66) Keskin, S.; Sholl, D. S. Assessment of a Metal-Organic Framework Membrane for Gas Separations Using Atomically Detailed Calculations: CO_2, CH_4, N_2, H_2 Mixtures in MOF-5. *Ind. Eng. Chem. Res.* **2009**, *48*, 914.

Table 1. Comparison of experiments[30] and model predictions for pure gas permeabilities (Barrers) of CO_2 and CH_4 in IRMOF-1/Matrimid MMMs.

Weight % of IRMOF-1	Experiments	Maxwell	Bruggeman	Lewis-Nielson	Pal	Modified Maxwell	Felske	Modified Felske
			CO_2					
0	9.00±0.1							
10	11.10±1.4	14.53	15.74	14.99	16.28	13.26	11.44	11.60
20	13.80±2.8	20.02	25.14	22.35	28.66	17.18	13.45	14.04
30	20.20±1.4	25.54	37.74	32.11	50.69	20.83	15.15	16.40
			CH_4					
0	0.22±0.02							
10	0.22±0.04	0.36	0.38	0.37	0.40	0.30	0.28	0.28
20	0.34±0.04	0.49	0.61	0.55	0.70	0.37	0.33	0.34
30	0.45±0.06	0.62	0.92	0.79	1.24	0.44	0.37	0.40

Table 2. Comparison of AARE% values for CO_2 and CH_4 permeation data in IRMOF-1/Matrimid MMMs

Permeation model	CO_2 AARE%	CH_4 AARE%
Modified Felske	8.37	13.60
Felske	10.20	16.04
Modified Maxwell	15.68	16.64
Maxwell	34.15	48.07
Lewis-Nielson	51.99	67.26
Bruggeman	70.25	86.94
Pal	101.76	120.89

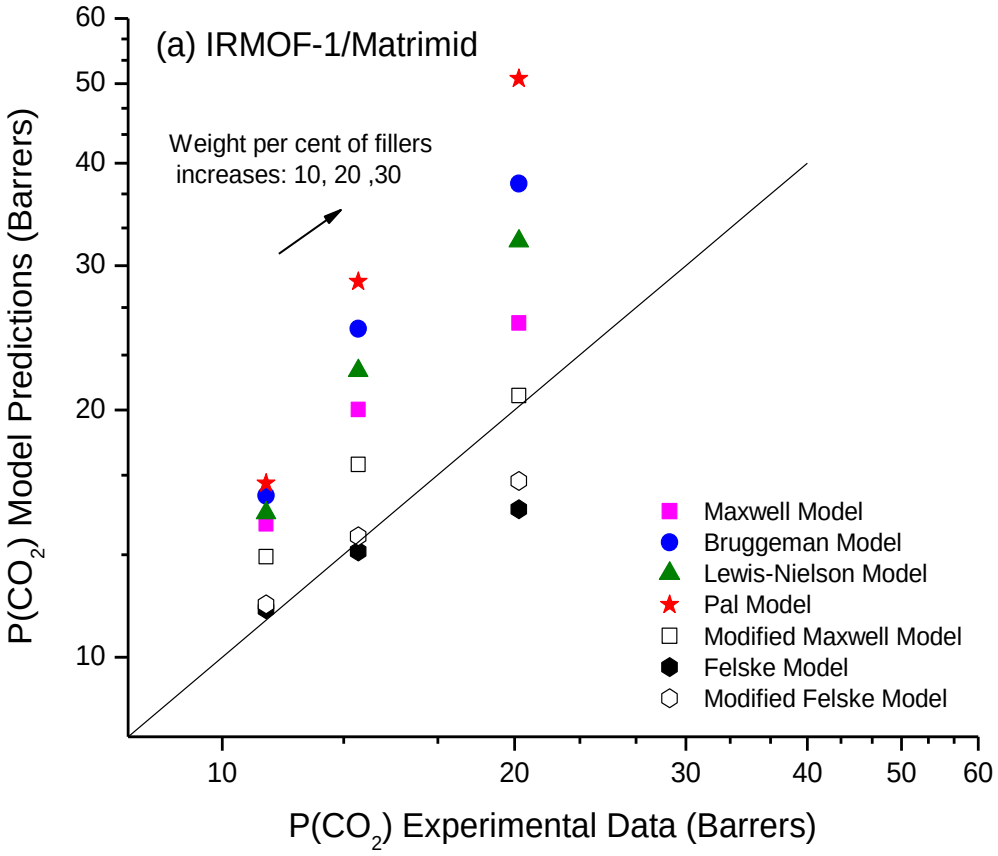
(a) IRMOF-1/Matrimid
Weight per cent of fillers increases: 10, 20 ,30
P(CO2) Model Predictions (Barrers)
P(CO2) Experimental Data (Barrers)
Maxwell Model
Bruggeman Model
Lewis-Nielson Model
Pal Model
Modified Maxwell Model
Felske Model
Modified Felske Model
10
20
30
40
50
60

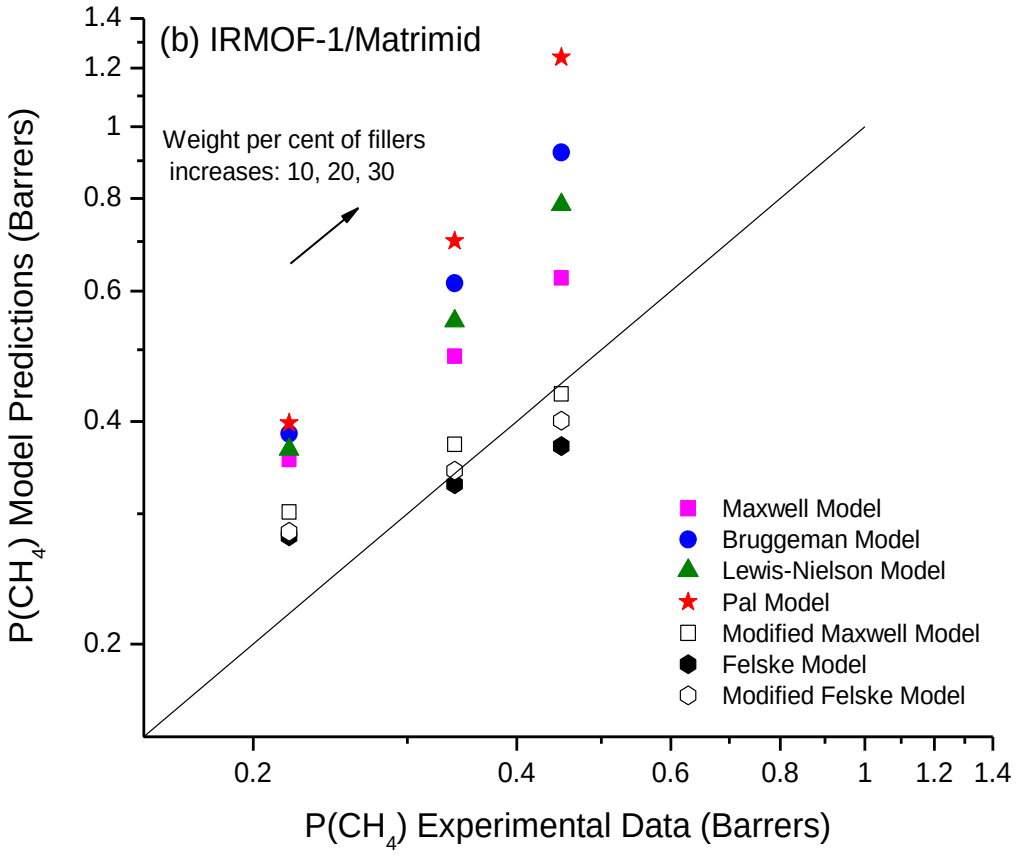
(b) IRMOF-1/Matrimid
Weight per cent of fillers
increases: 10, 20, 30
P(CH4) Model Predictions (Barrers)
P(CH4) Experimental Data (Barrers)
Maxwell Model
Bruggeman Model
Lewis-Nielson Model
Pal Model
Modified Maxwell Model
Felske Model
Modified Felske Model
0.2
0.4
0.6
0.8
1
1.2
1.4

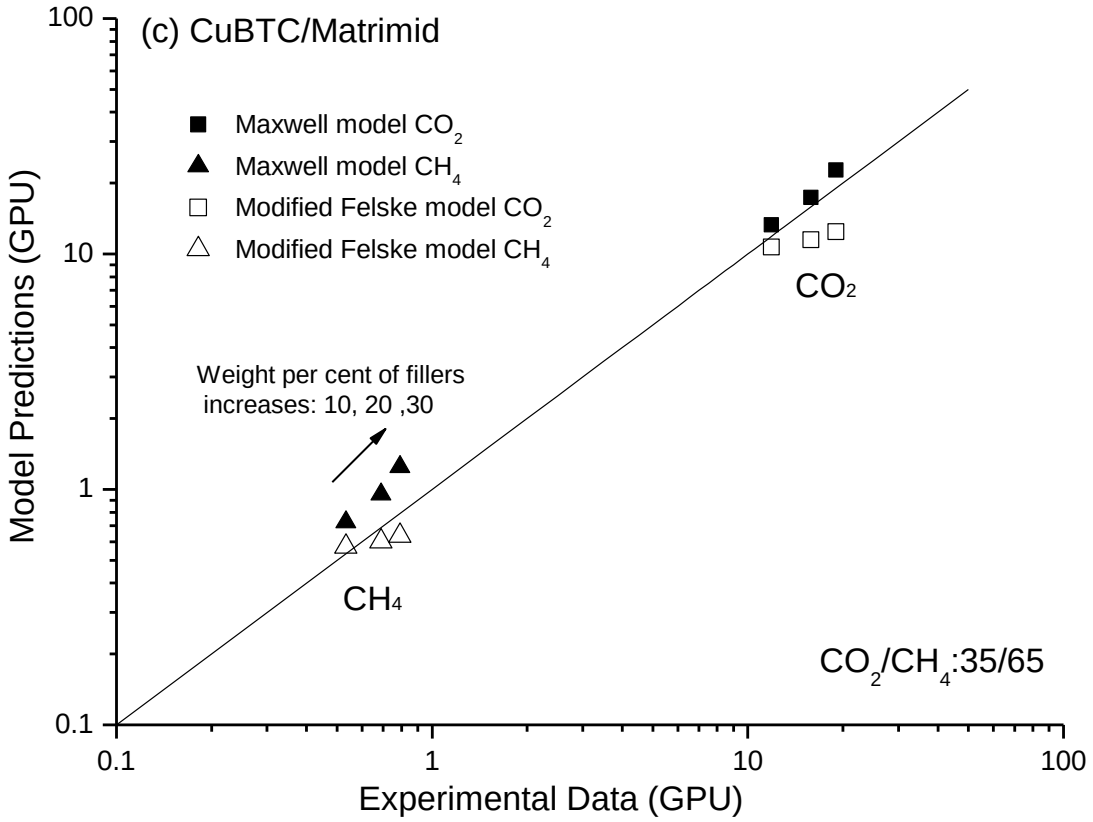

Figure 1. Comparison of pure gas permeabilities of a)CO_2 and b)CH_4 in IRMOF-1/Matrimid MMMs using different models. Experimental data is taken from Perez et al.[30] c)Comparison of mixed gas permeabilities of CO_2/CH_4:35/35 mixture in CuBTC/Matrimid MMMs. Experimental data is taken from Basu et al.[34](1 GPU = 1 Barrers/μm)

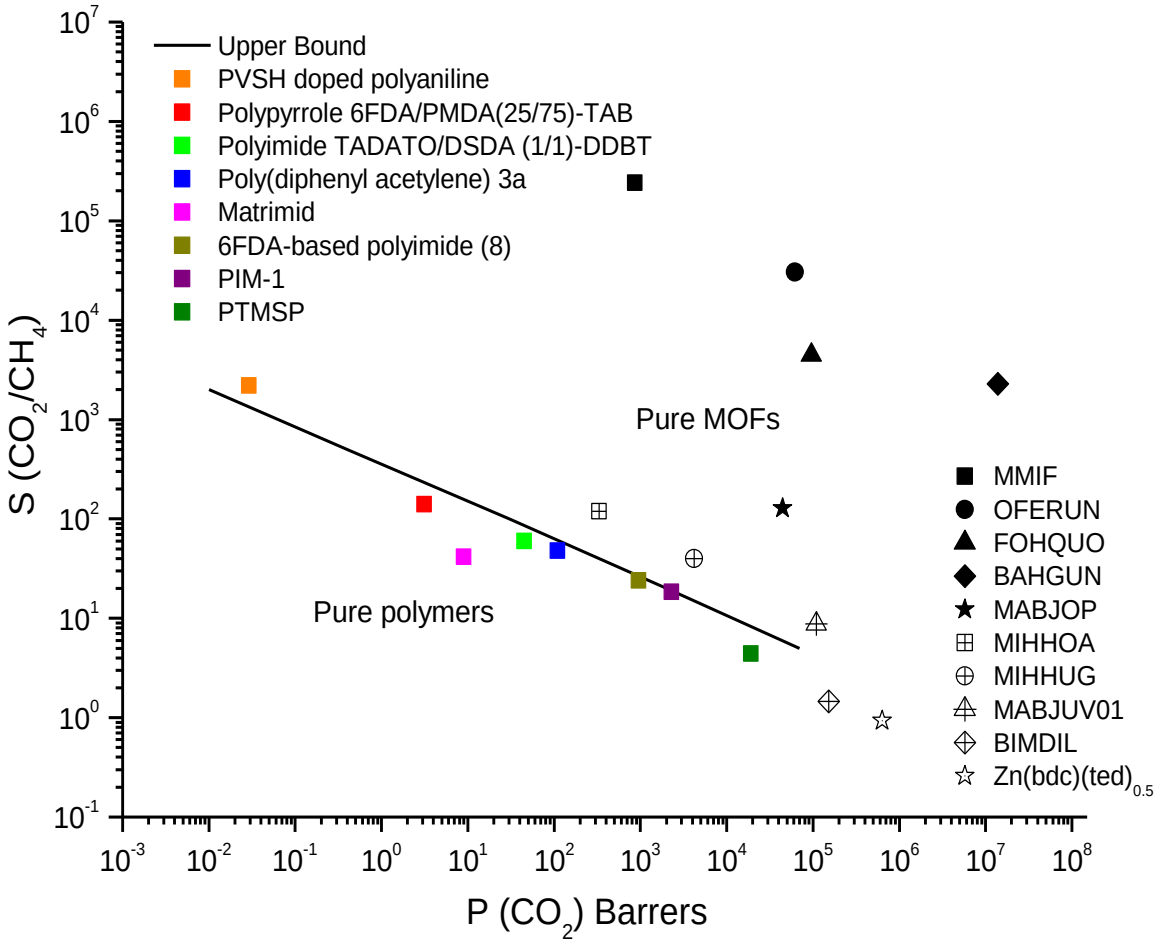

Figure 2. CO_2 selectivity and permeability of pure polymers and pure MOFs considered in this work.

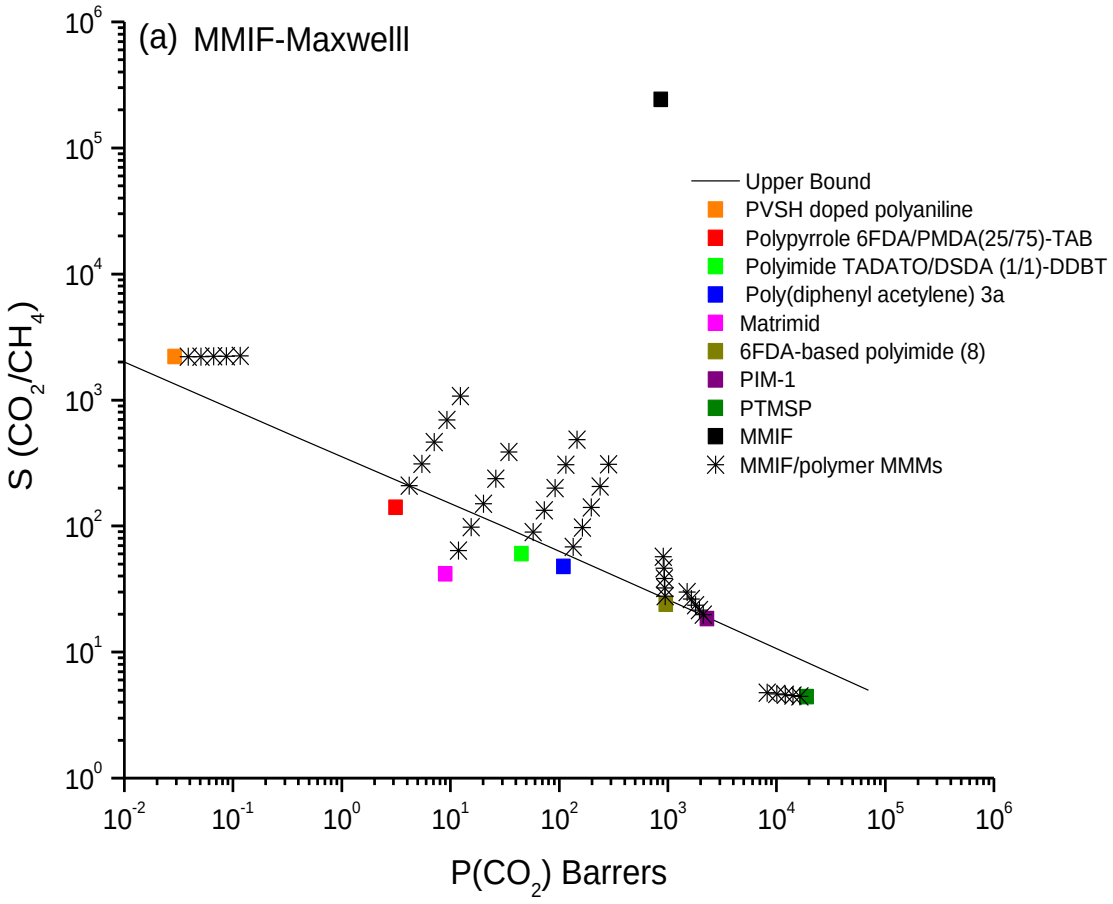
(a) MMIF-Maxwelll
S (CO2/CH4)
P(CO2) Barrers
Upper Bound
PVSH doped polyaniline
Polypyrrole 6FDA/PMDA(25/75)-TAB
Polyimide TADATO/DSDA (1/1)-DDBT
Poly(diphenyl acetylene) 3a
Matrimid
6FDA-based polyimide (8)
PIM-1
PTMSP
MMIF
MMIF/polymer MMMs

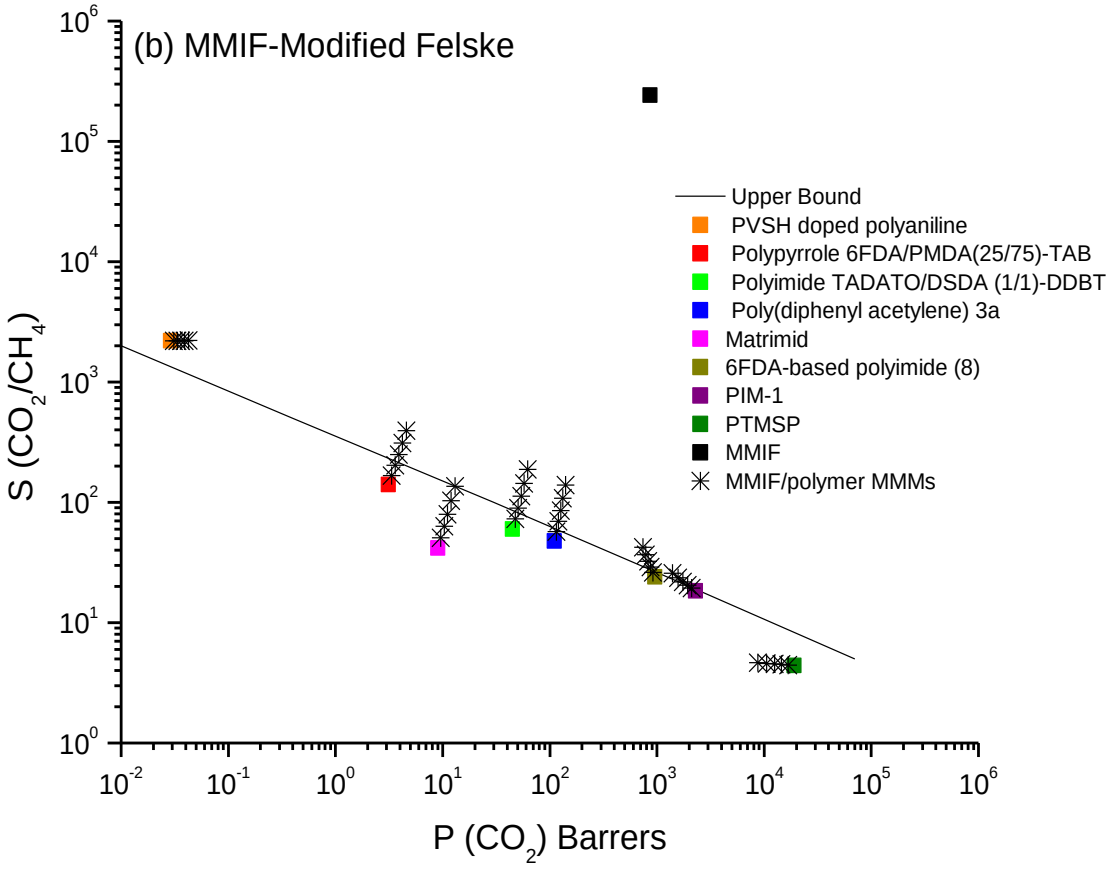
(b) MMIF-Modified Felske
S (CO2/CH4)
P (CO2) Barrers
Upper Bound
PVSH doped polyaniline
Polypyrrole 6FDA/PMDA(25/75)-TAB
Polyimide TADATO/DSDA (1/1)-DDBT
Poly(diphenyl acetylene) 3a
Matrimid
6FDA-based polyimide (8)
PIM-1
PTMSP
MMIF
MMIF/polymer MMMs

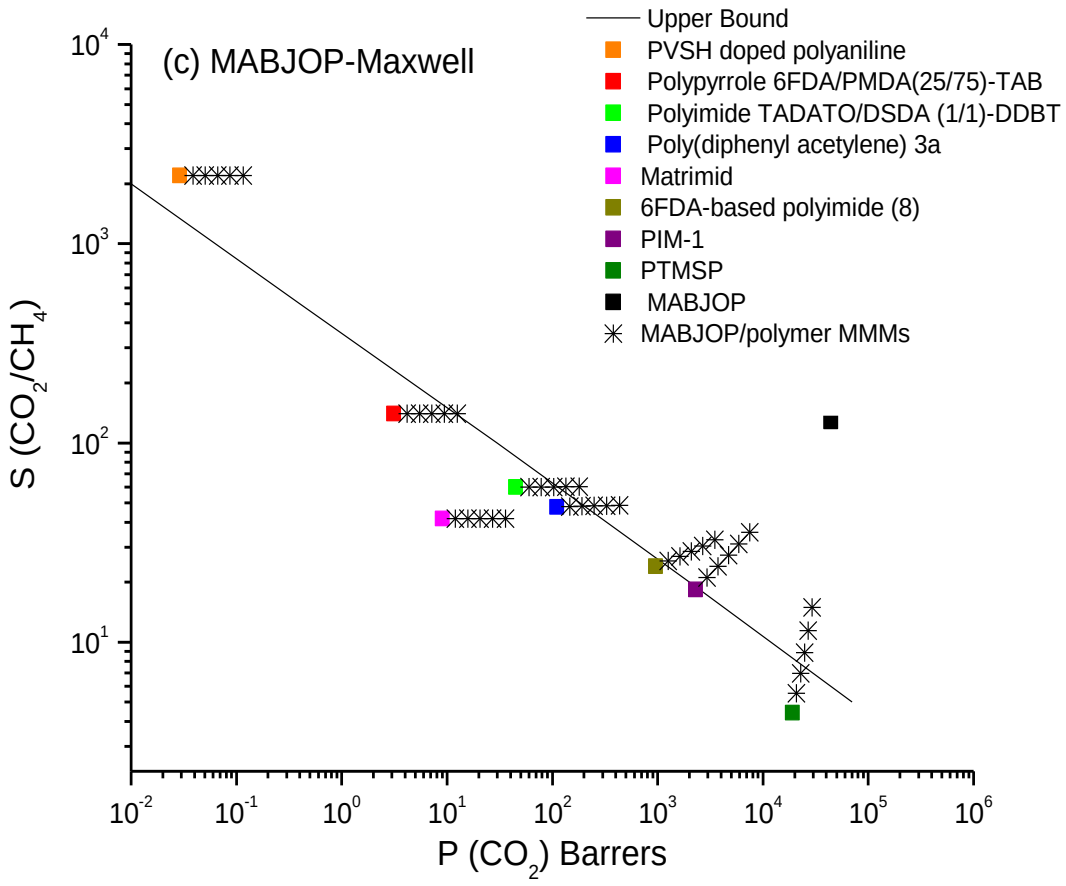
(c) MABJOP-Maxwell
Upper Bound
PVSH doped polyaniline
Polypyrrole 6FDA/PMDA(25/75)-TAB
Polyimide TADATO/DSDA (1/1)-DDBT
Poly(diphenyl acetylene) 3a
Matrimid
6FDA-based polyimide (8)
PIM-1
PTMSP
MABJOP
MABJOP/polymer MMMs
S (CO2/CH4)
P (CO2) Barrers

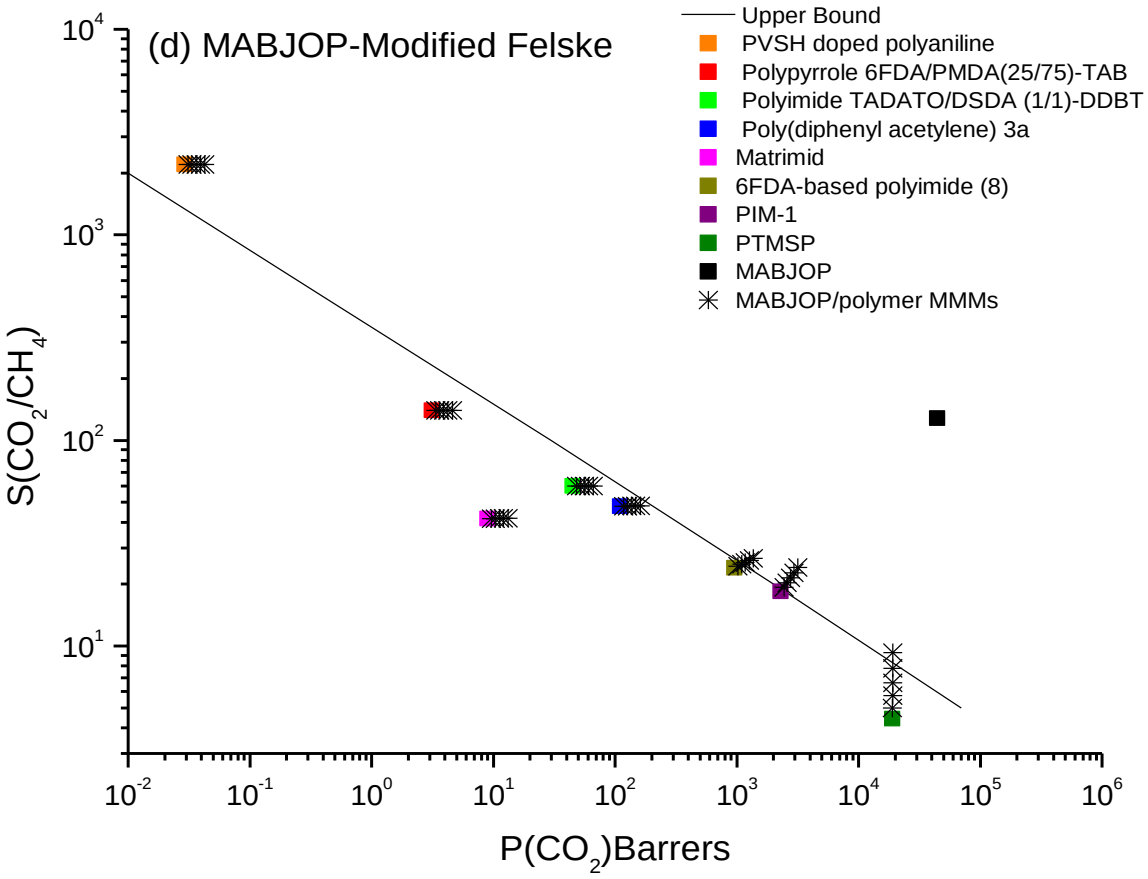
(d) MABJOP-Modified Felske
Upper Bound
PVSH doped polyaniline
Polypyrrole 6FDA/PMDA(25/75)-TAB
Polyimide TADATO/DSDA (1/1)-DDBT
Poly(diphenyl acetylene) 3a
Matrimid
6FDA-based polyimide (8)
PIM-1
PTMSP
MABJOP
MABJOP/polymer MMMs
S(CO2/CH4)
P(CO2)Barrers

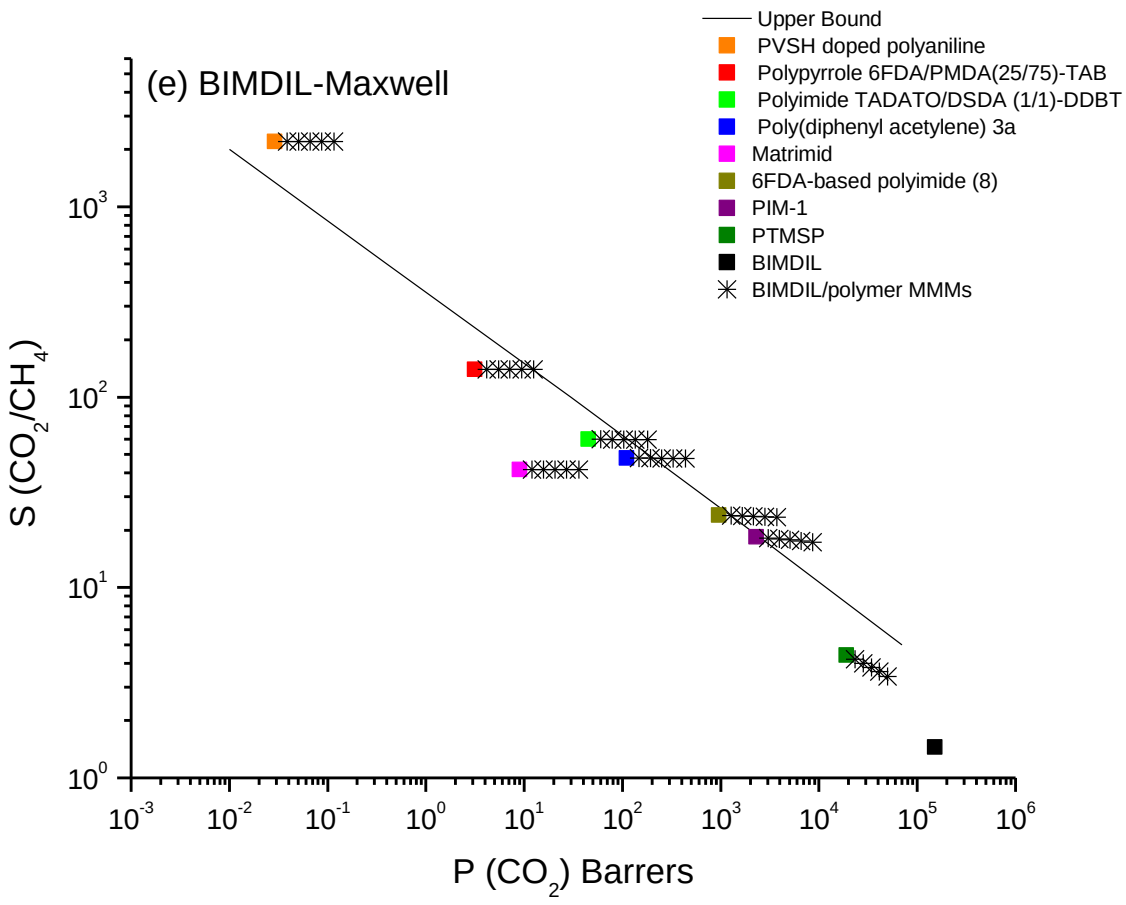
(e) BIMDIL-Maxwell
Upper Bound
PVSH doped polyaniline
Polypyrrole 6FDA/PMDA(25/75)-TAB
Polyimide TADATO/DSDA (1/1)-DDBT
Poly(diphenyl acetylene) 3a
Matrimid
6FDA-based polyimide (8)
PIM-1
PTMSP
BIMDIL
BIMDIL/polymer MMMs
S (CO2/CH4)
P (CO2) Barrers

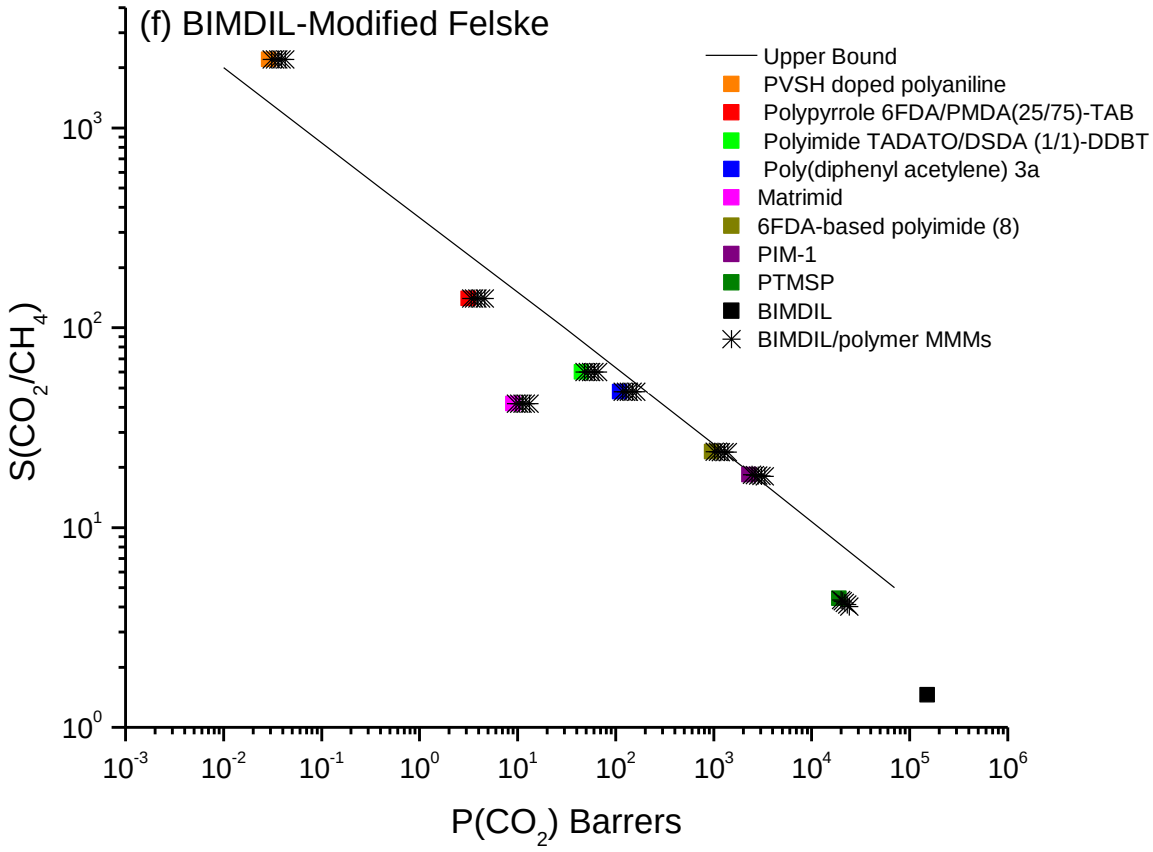

Figure 3. Maxwell model (a, c, e) and modified Felske model (b, d, f) predictions for CO_2 selectivity and permeability of MMMs having filler particles MMIF, MABJOP and BIMDIL, respectively. Squares represent the performance of pure polymers and pure MOFs, stars represent the performance of MMMs with filler particles having volume fractions of 0.1, 0.2, 0.3, 0.4 and 0.5.

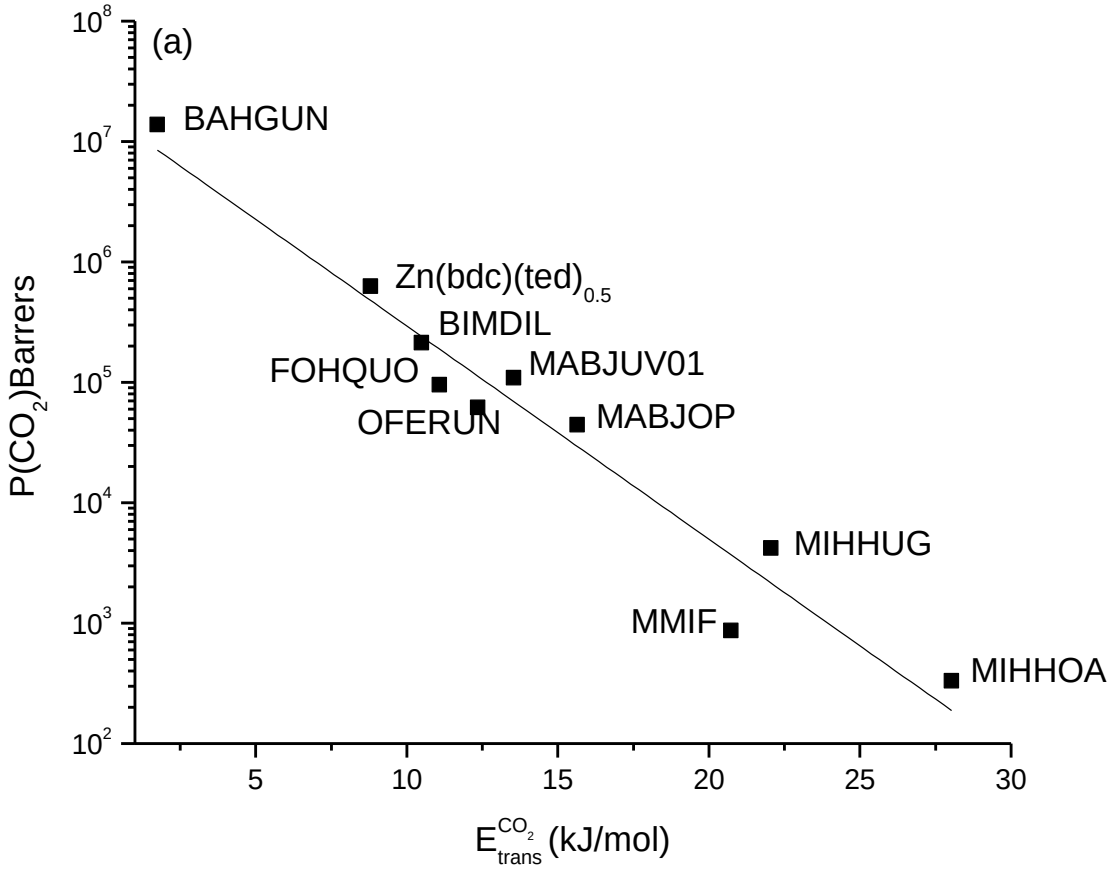
(a)
BAHGUN
Zn(bdc)(ted)0.5
BIMDIL
FOHQUO
MABJUV01
OFERUN
MABJOP
MIHHUG
MMIF
MIHHOA
P(CO2)Barrers
E trans CO2 (kJ/mol)
10^8
10^7
10^6
10^5
10^4
10^3
10^2
5
10
15
20
25
30

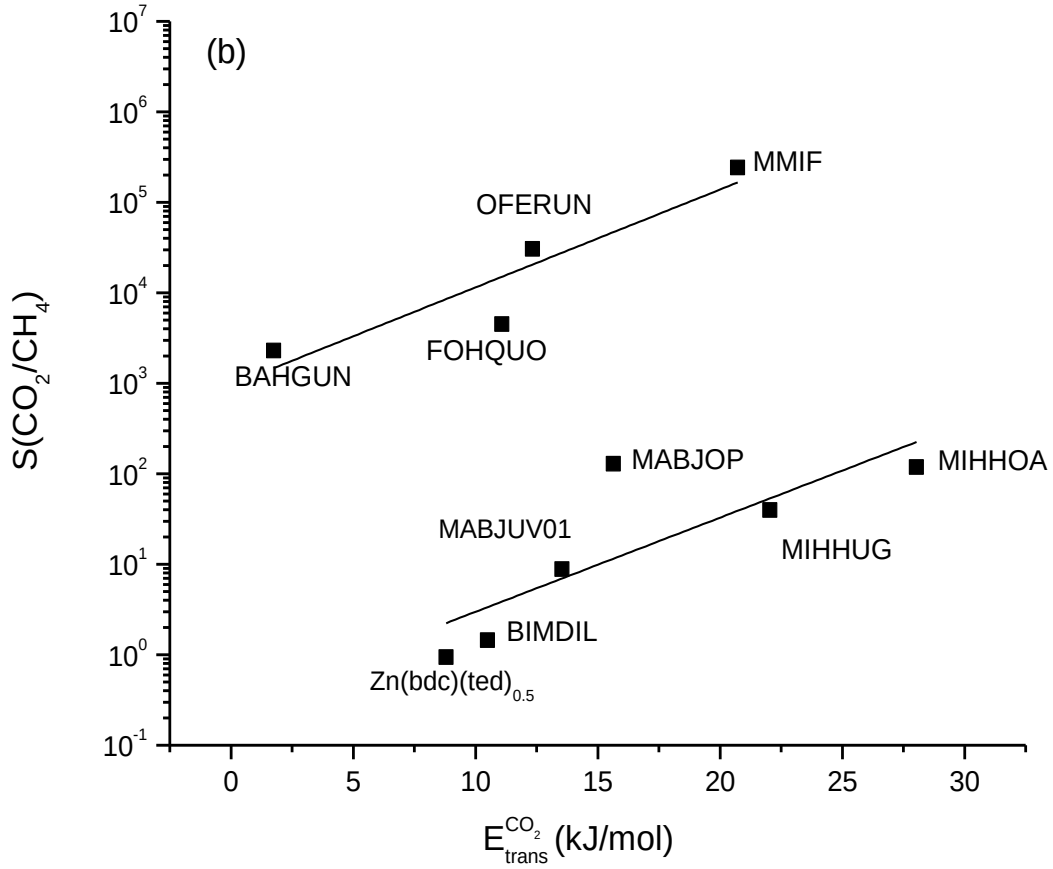

Figure 4. Relations between the energy barrier to CO_2 diffusion and a)CO_2 permeability b) CO_2/CH_4 selectivity.